

**Calculational Support for the Startup of the  
LEU-Fueled UMass-Lowell Research Reactor**

**John R. White, Justin Byard, and Areeya Jirapongmed**

**Chemical and Nuclear Engineering Department  
University of Massachusetts Lowell**

**Lowell, MA 01854**

**PHYSOR 2000**

**Pittsburgh, PA**

**May 7-11, 2000**

# **CALCULATIONAL SUPPORT FOR THE STARTUP OF THE LEU-FUELED UMASS-LOWELL RESEARCH REACTOR**

John R. White, Justin Byard, and Areeya Jirapongmed

Chemical and Nuclear Engineering Department  
University of Massachusetts Lowell  
Lowell, MA 01854

[John\\_White@uml.edu](mailto:John_White@uml.edu) [Justin\\_Byard@student.uml.edu](mailto:Justin_Byard@student.uml.edu) [Areeya\\_Jirapongmed@student.uml.edu](mailto:Areeya_Jirapongmed@student.uml.edu)

## **ABSTRACT**

The UMass-Lowell Research Reactor (UMLRR) is currently scheduled for conversion from high enriched uranium (HEU) fuel to low enriched uranium (LEU) fuel in the summer of 2000. One component of a larger effort to fully characterize the new LEU core was to provide computational support and guidance for the actual initial loading and for some of the tests required during the startup of the new LEU core. In particular, after some discussion of the models, methods, and data utilized in our calculations, this paper focuses on three key startup tasks: the initial critical core loading, the calibration of the control blades, and the evaluation of a variety of reactivity worths within the new LEU core. The data generated as part of these analyses provide a good estimate of the expected behavior of the new LEU core -- with particular attention to a variety of evaluations that will be performed during startup testing. The pre-planning performed here should serve as an invaluable guide when these tasks are actually performed during startup later this year.

## **INTRODUCTION**

The current core configuration at the UMass-Lowell Research Reactor (UMLRR) contains 28-30 high enriched uranium (HEU) fuel assemblies, most of which have been in use at the facility for roughly 25 years. However, a preliminary core configuration that uses only 20 low enriched uranium (LEU) fuel elements was designed several years ago,<sup>1-2</sup> and a particular configuration with 21 elements (19 full and 2 partial assemblies) of the same design was recently chosen as the final LEU startup core.<sup>3</sup> Since the Department of Energy (DOE) has recently given final approval for the manufacture of the new LEU fuel elements for the UMLRR, the new core should be fully operational by the second half of 2000 -- just in time to alleviate the need for additional new HEU fuel assemblies to maintain criticality of the current 25 year old core.

In preparation for the conversion to LEU fuel and a completely new arrangement for the fuel, graphite, and radiation basket assemblies, it was essential that an updated set of computational models specific to the LEU core be developed. To address this need, a major effort was undertaken to generate a wide range of computational models and analytical capabilities within the VENTURE,<sup>4</sup> DORT,<sup>5</sup> and MCNP<sup>6</sup> codes. In addition, since the deterministic codes require problem-specific effective cross sections, a set of broad-group LEU-specific cross sections for use in VENTURE and DORT were also developed. Our goal, of course, was to fully analyze and characterize the new LEU core to support the continued operation and use of the facilities within the UMLRR.

A particular component of this larger effort was to provide computational support and guidance for the actual initial loading and for some of the tests required during the startup of the new LEU core. In particular, this paper\* focuses on three key startup tasks: the initial critical core loading, the calibration of the control blades, and the evaluation of a variety of reactivity worths within the new LEU core. Both the critical loading simulation and the computation of the differential and integral blade worths follow, as closely as possible, the actual steps that are performed by the operations staff. In contrast, the reactivity worth evaluations simply involve a number of material perturbations to the reference computational models. Our goal in these analyses was to provide a reasonable prediction of expected behavior and to develop a procedure or sequence of steps for each startup task. The pre-planning performed here will be used as a guide by the operations staff when these tasks are actually performed during startup in the summer of 2000.

This paper first documents some of our initial cross section and model development work as background for the initial loading and reactivity worth computations. The three primary subjects of this paper, material worths, differential and integral blade worths, and the initial loading sequence, are then discussed in order. Finally, a brief summary and a note about future work conclude the paper.

## **DEVELOPMENT OF THE LEU CROSS SECTION LIBRARIES**

Generating effective group constants for performing reactor physics computations is a complicated process. Most 2-D and 3-D core and shielding calculations use the multigroup approximation and they use homogenized spatial regions to describe the real heterogeneous geometry of interest. The “effective” nuclear data used in such calculations must account for both the fine-group resonance effects and the real heterogeneous geometry of the system. This is achieved by performing resonance calculations to treat the spectral self shielding caused by large variations in the resonance cross sections and by performing assembly or cell calculations to account for the spatial self shielding associated with heterogeneous geometries. For the present work, these computations were accomplished with the BONAMI and XSDRN modules of the SCALE 4.3 system.<sup>8</sup> Other modules (such as AJAX, NITAWL, WAX, etc.) were also used to select appropriate isotopes from the base VITAMIN-B6 library,<sup>9</sup> to convert the cross section format to a form compatible with the different codes, and to merge individual isotopes into a final library for use in subsequent core calculations.

---

\* The reader is referred to Ref. 7 for a related paper that focuses on the characterization of the experimental facilities in the new LEU-fueled UMLRR.

The specific computations for the generation of the UMLRR LEU cross sections required a set of the three assembly calculations for the primary core elements -- one each for the full fuel assembly, partial fuel assembly, and control blade. These sequences treat the resonance self shielding for the specific isotope densities and geometries present in these elements, and they approximate the spatial self shielding with a detailed heterogeneous 1-D model of a unit assembly. The resultant effective cross sections, still at the fine-group level, are stored in the working library format<sup>8</sup> for subsequent use in XSDRN.

An infinite medium homogeneous model for the materials outside the fuel and control regions (water, aluminum, graphite, etc.) is also required. This calculation does not require an “assembly model” in XSDRN because the materials are actually contained in large homogeneous regions. Thus, the spatial self shielding that is associated with heterogeneous geometries is not of concern here. The resonance self shielding could still be important (for some isotopes) so the BONAMI step is still needed. The NITAWL code is also used here to convert the master library<sup>8</sup> output from BONAMI into the working library format for subsequent use in XSDRN.

The cross sections in the four individual libraries noted above were combined into a single working library using the WAX module of the SCALE 4.3 system. This working library, referred to as **leuxs.worlib**, still has the original fine-group representation (199 neutron groups and 42 gamma groups). This level of energy detail is suitable for 1-D core calculations, but it has too much fine structure for reasonable computational times for 2-D or 3-D models. Thus, a final XSDRN calculation, using a generic 1-D model of the reactor, was performed to determine a typical fine-group weighting function and to collapse the fine-group library to the broad-group level for subsequent multidimensional calculations. This step was performed twice -- once to give a 2-group library for relatively simple VENTURE diffusion theory calculations (used for computing  $k_{\text{eff}}$  and power distributions) and a second time to create a 47/20-group coupled neutron-gamma library for DORT transport theory analyses (typically used to determine neutron and gamma spectra in 2-D configurations -- as in Ref. 7). The cross sections output from this final XSDRN step are stored in the **leu2gxs.asnlib** and **leu67gxs.asnlib** ANISN-formatted libraries. These two libraries, after a little additional post processing, can be used for VENTURE and DORT computations, respectively.

In summary, the cross section generation procedure outlined above created three problem-specific nuclear data libraries that can be utilized in subsequent UMLRR LEU core analyses, as follows:

- leuxs.worlib** - 199/42-group working library for use with 1-D XSDRN core models<sup>8</sup>
- leu2gxs.asnlib** - 2-group data in ANISN format for 2-D or 3-D VENTURE models<sup>4</sup>
- leu67gxs.asnlib** - 47/20-group data in ANISN format for 2-D DORT calculations<sup>5</sup>

The **leu2gxs** library was the primary dataset utilized in the current study, since all the computations reported later in this paper involve calculations with various 2-D and 3-D VENTURE models. The **leu67gxs** library was used extensively in Ref. 7 where a variety of DORT calculations were used to quantify the radiation environment in the vicinity of the experimental facilities within the LEU-fueled UMLRR. Thus far, the XSDRN-based library, **leuxs**, has only been used as part of the cross section generation process described here. However, it can also be used in other related XSDRN calculations for the LEU core, as desired.

## THE VENTURE 2-D AND 3-D LEU CORE MODELS

The UMass-Lowell Research Reactor (UMLRR) contains a 9x7 grid of fuel assemblies, graphite reflector elements, radiation baskets, and corner posts. It also has two grid locations reserved for an external neutron source and a low-worth regulating rod for fine reactivity control. Four large control blade assemblies are used for gross reactivity control and for flux shape adjustments. From the top view, the reactor is enclosed by an aluminum core box and a large pool of demineralized water surrounds the system on three sides, with a 3 inch lead shield and large graphite thermal column on the remaining side. A specific arrangement of fuel elements, graphite reflector blocks, and radiation baskets make up a particular core configuration.

The basic layout for the proposed reference LEU core arrangement, including the beam ports and thermal column, is sketched in Fig. 1. The reference configuration contains 19 full fuel assemblies and 2 partial assemblies arranged roughly in the center of the 9x7 grid. Directly in the middle of the core is a central irradiation zone known as the flux trap. The flux trap is similar to a radiation basket, except that the region between the inner irradiation tube and the outer aluminum can is filled with graphite.

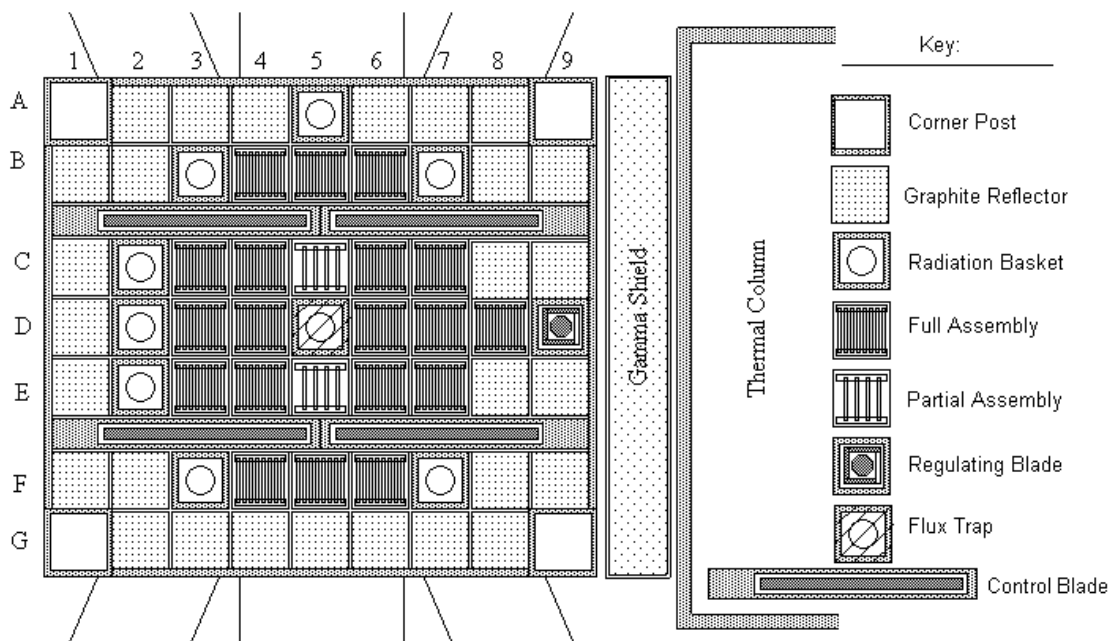


**Fig. 1 Rough sketch of the reference LEU core configuration for the UMLRR.**

Putting together a computational model for any reactor system requires precise information about the geometry and material composition of the actual system. It also requires a number of decisions by the model builder concerning the mesh grid layout, the zone placement, and the degree of detail that can be modeled efficiently and accurately within the limitations of the available computer tools. These decisions often require that tradeoffs be made in the model details, and these usually result in the consolidation of the fine heterogeneous geometry details into larger homogeneous regions. The homogeneous zones must use properly averaged material

densities to approximate the actual materials present in the real system. They also require a problem-dependent set of microscopic cross sections that account for the heterogeneous detail that is lost when developing a homogeneous model -- and the procedure for the generation of a suitable library was discussed in the previous section.

### **The 2-D VENTURE Model**

In the current 2-D model, each interior grid location within the UMLRR geometry (the central 7x5 grid array) was broken into a 5-region, 3-zone symmetric configuration. Each grid location has two sides (top and bottom), two edges (left and right), and a center region. This zone layout and the specific dimensions used are consistent with the LEU fuel assembly geometry (see a detailed description in Refs. 1 and 2). This arrangement allows explicit modeling of the side plate and central fueled regions of the fuel assembly. It also allows for treatment of the aluminum end plates and the slightly increased water content associated with the assembly gap. This explicit 5-region, 3-zone model for each interior grid location is apparent in the LEU215 configuration shown in Figs. 2 and 3 -- Fig. 2 shows the full 2-D model geometry and Fig. 3 displays an expanded view of the core region for better resolution of some of the modeling details incorporated into the 2-D model. The remaining structures (control blades, corner posts, lead shield, thermal column, beam ports, etc.) are also displayed explicitly in these diagrams.

Getting the actual geometry and homogenized material information into the VENTURE code requires specification of three key arrays: a region grid layout, a zone-by-region map, and a material-by-zone array. The current 2-D model uses a 69x67 region layout and a fine-mesh grid containing 175x170 mesh points, spanning 225 cm in the x direction and 200 cm in the y direction.

A zone-by-region map is then given which identifies a specific zone number with each region in the 2-D grid structure. For the current model, the zone numbers range from 1 to 189 (for ease in modeling, a few zones numbers were not used). Attention to detail in specifying the zone and mesh map allows one to build a relatively flexible geometry that can handle a variety of material configurations. This modeling step is quite important, because a little added flexibility here can save lots of analysis time if several material layouts need to be considered.

The final zone-by-region map for the current model was passed through a short Matlab program called Plot\_Vgeo to plot the resultant zone layout and the material map for a specific configuration. The result of this exercise gave the zone and material maps for the LEU215 configuration shown in Figs. 2 and 3. This process helps to debug the geometry setup and to visualize the details of the final model.

Note, for example, that the four angled beam ports in the UMLRR were modeled with a relatively coarse stair-step approximation to minimize the number of region boundaries specified within VENTURE. Since the regions of interest in all our anticipated studies occur within the core or at the beam port/core box interface, the jagged edges used to represent the beam port sides should not seriously affect subsequent analyses. Thus, less detail can be incorporated, where appropriate, to simplify the model-building process.

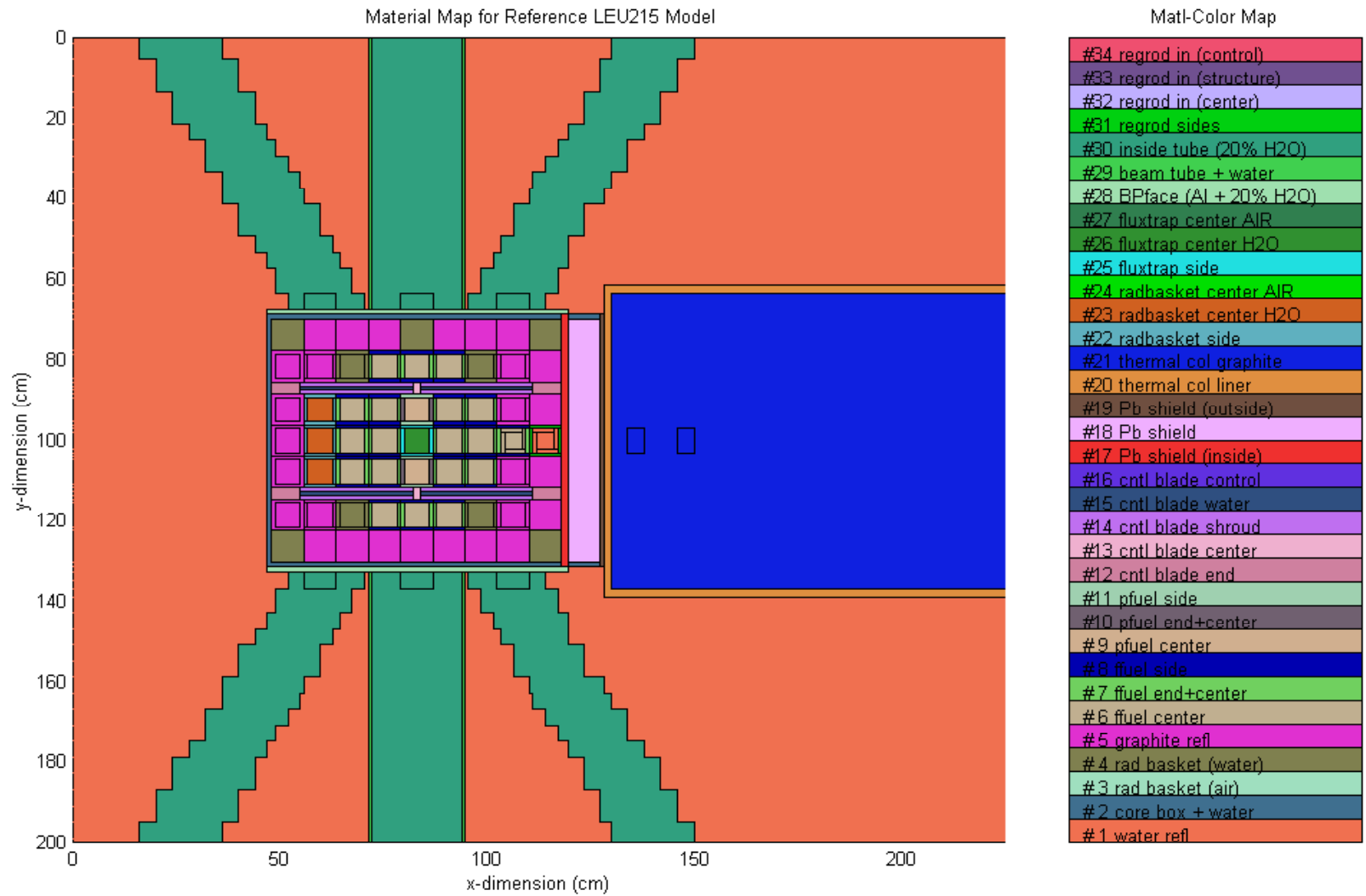


**Fig. 2 Material/zone map for the reference LEU 2-D XY calculational model.**

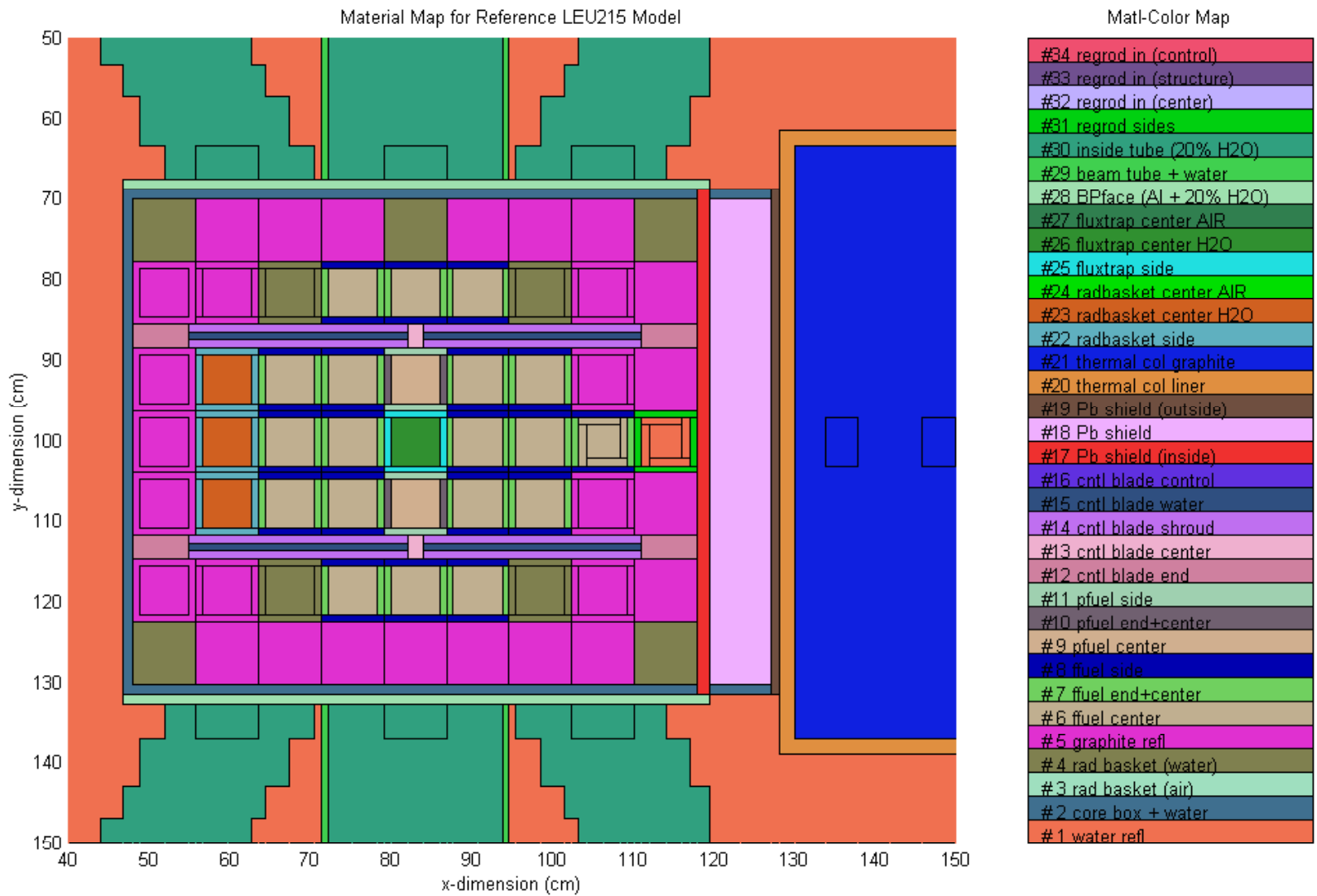


**Fig. 3** Expanded view of the core region for the reference LEU 2-D XY calculational model.

### The 3-D VENTURE Model

We have also developed a detailed 3-D VENTURE model of the LEU core as part of this overall study. The model has the same 69x67 planar region resolution as the 2-D model, but the 3-D computational model incorporates 17 axial planes that allow a relatively detailed axial representation for control movement (12 positions), fuel burnup (5 axial regions), and irradiation sample sizes and axial locations (8 axial zones). The current model has a 130x121x65 mesh grid in the three coordinate directions (over 1 million mesh points total), and 947 different zones allow considerable flexibility in the various material configurations that can be treated. The 3-D model also has the capability to place the regulating rod in either the D8 or D9 grid location, and explicit treatment of the flux trap irradiation region has been included. The definition of several edit regions to allow characterization of the experimental facilities for different arrangements of fuel elements and graphite and water reflector assemblies, and extra zone detail in the six grid positions (C1-C2, D1-D2, and E1-E2) for characterization of enhanced irradiation facilities (in the future) have also been added to the base 3-D model. Overall the 3-D VENTURE model is quite flexible -- and hopefully it can serve as a focal point for startup planning, operational support, and core follow/burnup analyses for the LEU core for the foreseeable future.

Because of the complexity involved in the 3-D model, the Plot\_Vgeo code was essential as a geometry-debugging tool. This program allows one to plot a combination zone and material map for any XY, XZ, or YZ plane within the model. Three such pictures from the LEU315crit configuration are given in Figs. 4-6 as examples of its plotting capability and also to illustrate the level of detail that is treated in the overall 3-D model. These three cuts are taken near the core midplane in each of the respective three directions. Note that this model has the control blades at the 16.5 inches withdrawn position -- which represents the critical state for this model. Any other row (y location for XZ cuts), column (x location for YZ cuts), or layer (z location for an XY view) can also be chosen to help visualize the full geometry model and material layout.

On option, Plot\_Vgeo can also write a significant portion of the actual VENTURE input file. This feature has saved countless hours of VENTURE input preparation and debugging -- and it works equally well for both the 2-D and 3-D models. Thus, Plot\_Vgeo represents a significant enhancement in our ability to generate base models and to modify existing models in a more efficient manner.

In addition to a flexible geometry, one also needs to specify a particular material composition to be placed in each zone (i.e. the so-called material-by-zone map). Homogenized atom densities for 34 materials were computed for the 2-D model based on the nominal region densities and region volume fractions within the given homogeneous zone. These materials include the primary core and reflector components (fuel, radiation baskets, graphite reflectors, core box, water reflector, flux trap, etc.) as well as mixtures that represent the excor structures as described by a 2-D geometric model. An additional 5 materials to account for various axial reflector zones were also needed for the 3-D model. The material-by-zone maps for the reference control-out 2-D model and the just-critical 3-D model can be seen in Figs. 2-6.

The geometry and material composition information make up a large part of the actual VENTURE input file. With the addition of suitable boundary conditions, the system power level, and specification of a few switches to set various code options, the model building process is complete. One is now ready to do the actual neutronics calculations in the VENTURE code.

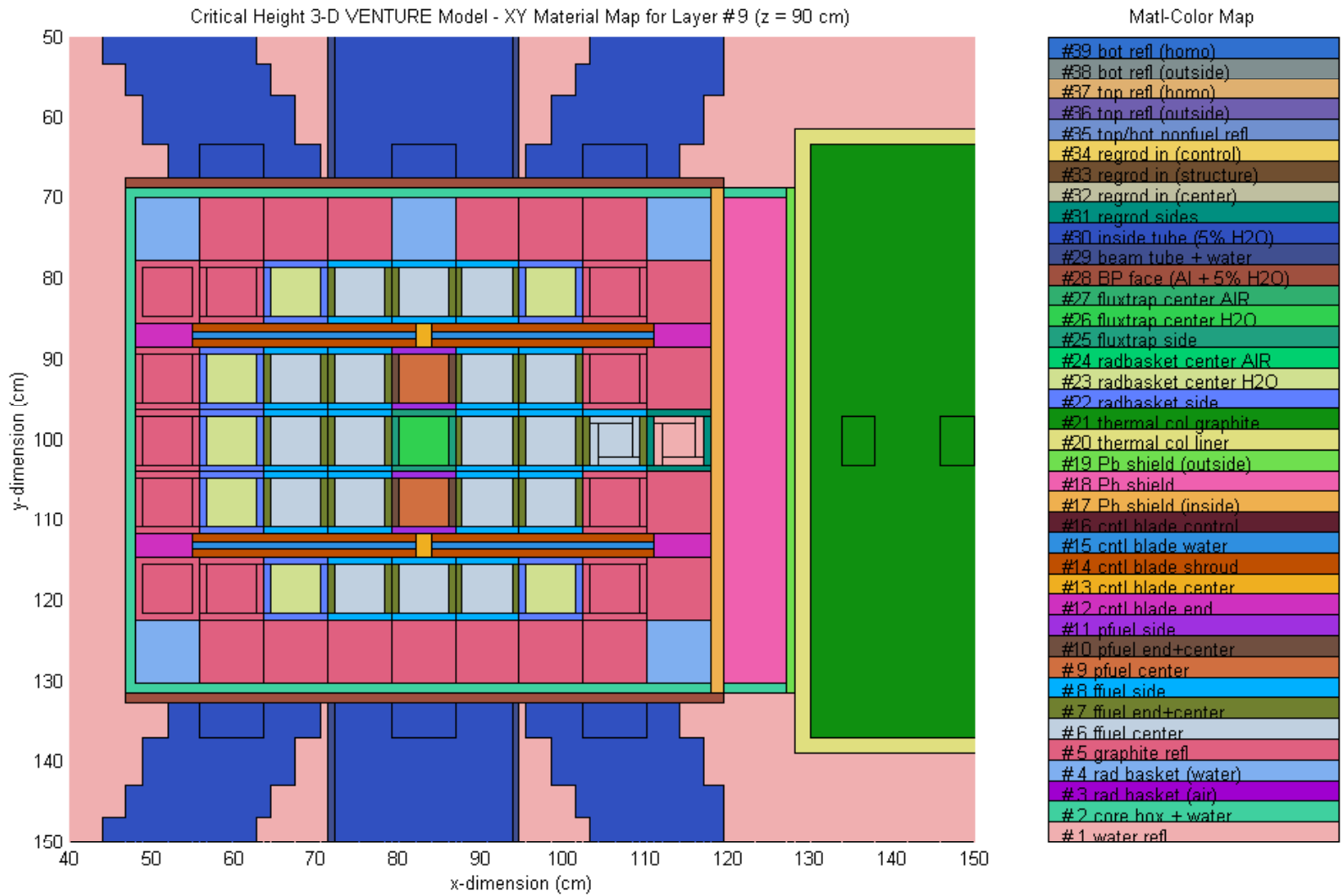


**Fig. 4 XY zone/material map near the core midplane for the LEU315crit model.**

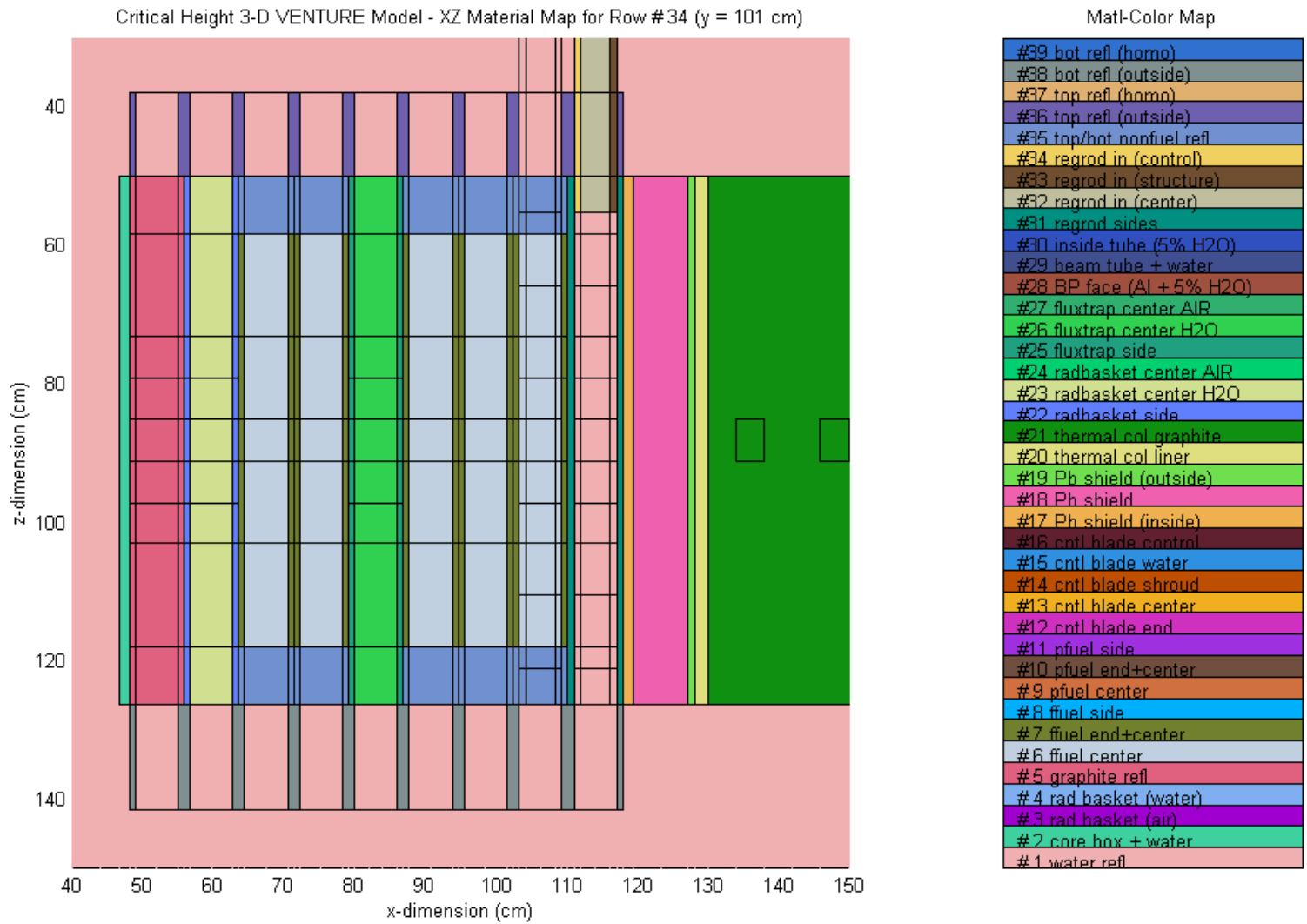


**Fig. 5 XZ zone/material map near the core midplane for the LEU315crit model.**

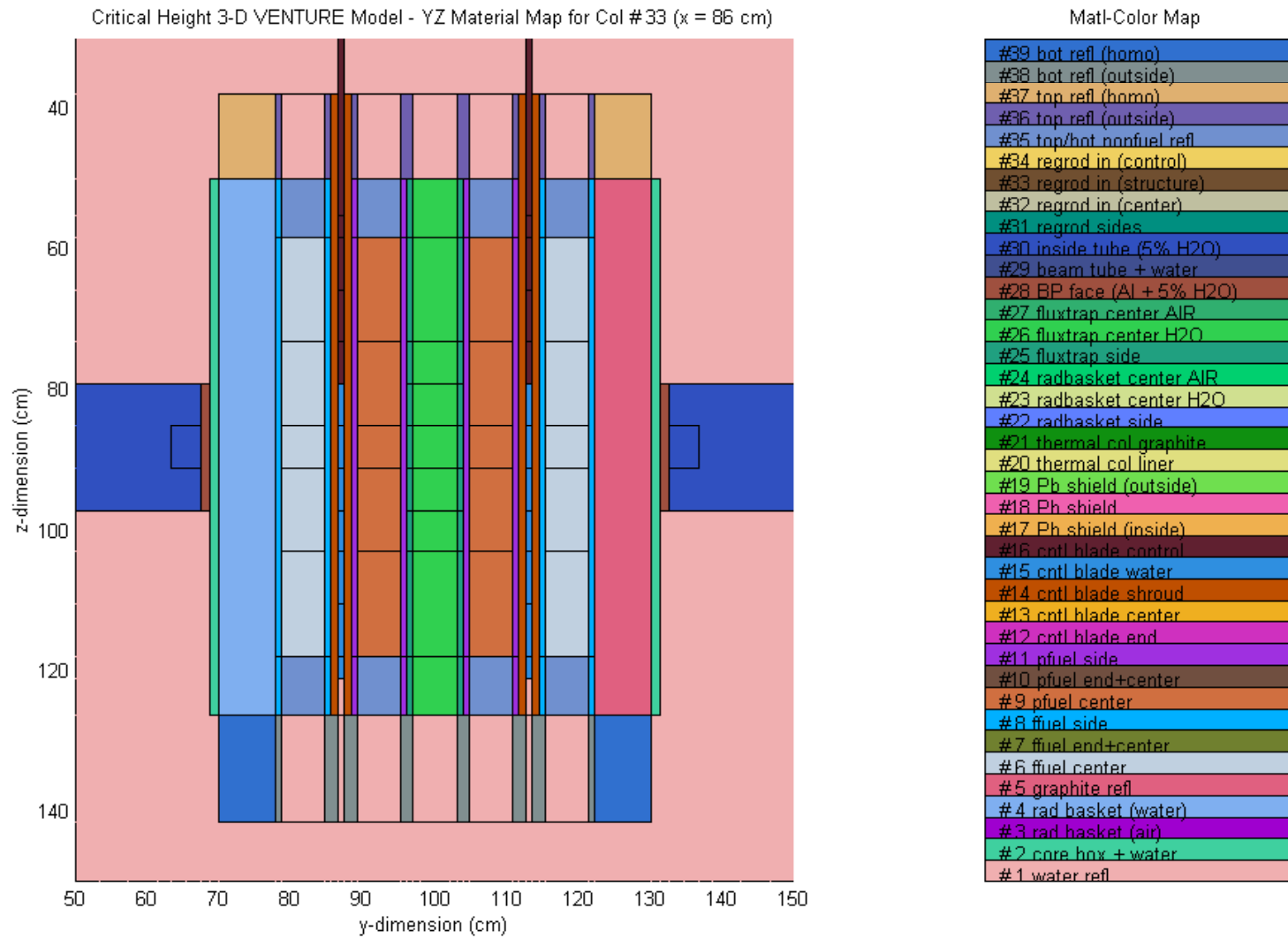


**Fig. 6** YZ zone/material map near the core midplane for the LEU315crit model.

## SUMMARY REACTIVITY AND INTEGRAL BLADE WORTH DATA

Using the base VENTURE models discussed above, a series of calculations was made to determine the initial excess reactivity and the total blade worths for the reference 21-element LEU-fueled UMLRR. In addition, the total worths derived from a set of integral worth curves (see next section) provide a good consistency check with the simple in-out worth results highlighted here. All this integral worth information, along with some additional material worth results, is summarized in this section. Note that, in all cases, the 2-D LEU215 and 3-D LEU315 models with the blades in their fully-withdrawn positions are treated as the reference configuration for the worth measurements. This choice is the only practical reference case for the 2-D models, but the 3-D geometry offers other options -- such as the just-critical LEU315crit case. However, for consistency, we decided to determine all the material worths relative to the all-blades-out configuration.

Table I presents much of the summary reactivity worth information associated with the reference LEU215/LEU315 VENTURE models. Some of the worths were computed with the 3-D model, but many of the table entries -- like the individual blade worths -- can be estimated quite accurately in 2-D XY geometry. Thus, the 3-D column is not complete and, where appropriate, the 3-D worths can be assumed to be approximately the same as the worths computed with the 2-D model. In these cases, the words "about same" are inserted into the 3-D column. Note also that all the data here were computed with the VENTURE 2-group cross section library generated specifically for this study (as discussed above).

From Table I we see that the best estimate of initial excess reactivity with the reference LEU 21-element core is roughly  $3.2 - 3.7\% \Delta k/k$ . This range is well within the upper design limit of  $4.7\% \Delta k/k$ , yet it represents sufficient excess reactivity for routine operation of the facility over a relatively long period of time.<sup>10</sup> Additional positive reactivity to counteract burnup effects can be achieved quite easily by moving the partial assemblies to lower worth locations, by replacing the partial elements completely with full fuel assemblies, or by simply replacing the four water baskets in the B3, B7, F3, and F7 locations with graphite reflector blocks. The worth associated with exchanging the four water baskets with graphite reflector assemblies, for example, is about  $1.2 - 1.4\% \Delta k/k$ . The other moves suggested above also represent large reactivity increases as seen in Table I. Thus, we expect that the base 21-element core configuration, with only minor modifications, will be the operating arrangement for quite a while.

Also given in Table I are the total control blade and regulating blade worths and the computed shutdown margin for the reference core. The first two columns of blade worths (for the 2-D and 3-D models) are computed using the difference in  $k_{\text{eff}}$  values for the blade-in versus blade-out configuration, with all the other blades fully withdrawn. The last column of blade worth data are derived from the integral blade worth curves using the combined cubic polynomial plus sinusoid as a mathematical model for the curve fitting program -- see a more detailed discussion below. Of interest here is the fact that the integral curve comes from a bottom-peaked differential worth distribution. However, it appears that the additional worth in the bottom just about offsets the reduced worth at the top, giving a total worth that agrees reasonably well with the simple in-out 2-D calculation given in the first column of Table I. This good agreement (about 3 - 5% differences in the  $\% \Delta k/k$  values) gives additional confidence in this whole series of computations.

**Table I Summary reactivity results for the reference LEU configuration.**

Calculated Worths* (% $\Delta k/k$ )	VENTURE 2-D model	VENTURE 3-D model	Data from integral worth curves
<b>Excess Reactivity</b>			
Initial excess reactivity	3.26	3.67	---
PAs in C5+E5 moved to C4+E4	0.61	about same	---
PAs in C5+E5 moved to C3+E3	1.27	about same	---
PAs in C5+E5 replaced by FAs	2.07	about same	---
4 water baskets replaced with graphite reflectors	1.20	1.36	---
<b>Blade Worths and Shutdown Margin</b>			
Blade 1 worth	2.68	2.66	2.71
Blade 2 worth	2.62	about same	2.78
Blade 3 worth	3.30	about same	3.41
Blade 4 worth	3.37	about same	3.50
Total blade worth	12.0	about same	12.4
Worth of flooded beam ports	---	0.44	---
Shutdown margin	4.40	3.99	4.29
Regulating blade worth	0.39	about same	0.40
<b>Sample Worths</b>			
Standard sample in D2	---	0.07	---
Standard sample in D5	---	0.37	---
<p><b>*Notes:</b></p> <ol style="list-style-type: none"> <li>1. PA and FA refer to partial and full fuel assemblies, respectively.</li> <li>2. The computed shutdown margin is probably conservative because the flooded beam port worth estimate is higher than the expected measured result.</li> <li>3. The tabulated regulating blade worth includes a 20% reduction to account for expected uncertainties in the VENTURE models. Actual computed values are 1.2 times the values shown. The estimated uncertainty is from Ref. 3.</li> <li>4. The standard sample worths are expected to be very high relative to measured values because the high-worth sample is smeared over a large area relative to its actual physical size.</li> </ol>			

As apparent from Table I, Blades #1 and #2 are worth less than Blades #3 and #4. This is due primarily to the asymmetry associated with having a full fuel assembly in the D8 grid location (see Fig. 1, for example). However, this asymmetric blade distribution is quite consistent with the distribution observed in the current HEU core. Thus, routine operation of the facility should not be adversely affected by this mild asymmetry.

Note that the tabulated results for the VENTURE-calculated regulating blade worths have already been reduced by an expected uncertainty of roughly +20%. For example, the reported value of 0.39%  $\Delta k/k$  in Table I was computed as 0.47%  $\Delta k/k$ . This bias is the result of the spatial homogenization approximations used when the VENTURE models were first developed. We have decided to report the total regulating blade worths in this fashion because this estimated worth is expected to be much closer to the actual value that will be observed in the physical system. A preliminary MCNP model of the LEU-fueled UMLRR was used to obtain the rough estimate of the uncertainty in this particular VENTURE calculation.<sup>3</sup> Even with this estimated uncertainty applied to the calculated results, the predicted D9 blade worth for the new reference core satisfies the imposed design constraint of 0.35%  $\Delta k/k$  as the minimum acceptable worth.

The shutdown margin is a measure of the amount of subcriticality that is achievable under worse case conditions. We define worse case here assuming that the beam ports are flooded (0.44%  $\Delta k/k$ ), that the maximum experimental worth of +0.5%  $\Delta k/k$  is inserted,<sup>10</sup> and that the most reactive blade (Blade #4 with a worth of 3.4 - 3.5%  $\Delta k/k$ ) is stuck out. Adding these positive contributions to the excess reactivity and subtracting the total blade worth gives an estimated shutdown margin of about 4.0 - 4.4%  $\Delta k/k$ . This is well above the technical specification limit of 2.7%  $\Delta k/k$ .<sup>10</sup>

Our estimate of the shutdown margin is expected to be somewhat conservative because the VENTURE-computed flooded beam port worth is probably quite large relative to the worth in the real system. Our treatment of the voided beam ports in the 3-D VENTURE diffusion theory model, for example, was very crude, and certainly the results obtained using this model only represent a rough approximation to reality. The measured worth of the flooded beam ports for the HEU core was about 0.15%  $\Delta k/k$ .<sup>11</sup> We expect the worth in the LEU core to be slightly higher because of the greater leakage fraction associated with the smaller core (probably 0.15 - 0.20%  $\Delta k/k$ ). Thus, the VENTURE-computed value for the flooded beam port worth is probably high by a factor of two or more.

Table I also shows some approximate worths associated with an experimental sample placed in the radiation basket in position D2 and in the flux trap in grid location D5. The sample here was assumed to be a 45-mil thick (0.1143 cm) borated aluminum plate curved into the shape of a hollow cylinder. The cylinder is 2.36 inches in length (6 cm) and the inside diameter is 1 inch (2.54 cm). This small sample was placed in the axial midplane of the reactor (Level 9 in the LEU315 model) and the worth relative to the experiment-free configuration was computed. Although the axial location is modeled accurately, our planar 2-region basket model requires that the sample be homogenized within the inner region of the basket model. This introduces a large uncertainty, since smearing a poison material over a much larger area (with a lower density, of course) usually leads to a large over-prediction of the poison worth. Here, with a real sample volume fraction of less than 2%, we expect that the estimated worths will be very high.

Although the model deficiency noted above implies that the values of absolute computed worths are not very reliable, it is expected that the relative worth from position D2 to D5 will be a reasonable prediction of the increase that can be expected in the real system. From Table I we see that, as expected, the worth of the same sample in D5 is much greater than in D2 (0.37%  $\Delta k/k$  versus 0.07%  $\Delta k/k$ , respectively). This rough factor of 5 increase in worth in the flux trap relative to a radiation basket on the core periphery is reason for concern, since the current technical specification limit for any movable experiment is only 0.1%  $\Delta k/k$ .<sup>10</sup> Thus, it is possible that a sample that easily meets the worth criterion for use in the radiation basket may not be appropriate for irradiation within the flux trap facility. For normal operation of the new LEU core, a good estimate of the reactivity worth of new experiments placed within the flux trap will have to be carefully estimated prior to use and the actual worth will need to be monitored during operation -- so that the technical specifications for a movable experiment are not violated.

### DIFFERENTIAL AND INTEGRAL WORTH CURVES

One of the first tasks that will be required as part of the startup tests for the new LEU core is the calibration of the four large control blades and the regulating blade. Differential and integral worth curves are usually generated experimentally in conformance to an in-house special procedure. This procedure outlines the experimental technique used for gathering the necessary differential reactivity worth data and it suggests that the data be fit to a simple theoretical model given by

$$\frac{d}{dz} \rho(z) = a_1 \left( 1 - \cos \left( \frac{2\pi z}{H} \right) \right) \quad (1)$$

where H represents the full range of the blade in inches (H = 26 inches for the UMLRR) and z gives the blade position in inches withdrawn. This mathematical representation is derived from a very simple bare homogeneous 1-group diffusion theory model of the system. In addition, it assumes that only one control blade is present in the reactor. Equation (1) and its integral lead to the familiar symmetric “bell-shaped” differential blade worth curves and to the symmetric “S-shaped” integral blade worth curves that can be seen in most reactor theory texts.<sup>12</sup>

Although this simple conceptualization of a typical differential and integral worth curve is an excellent tool for a basic understanding of the physics involved, it was never really intended to be used as a quantitative predictive tool for a real operating reactor. Its biggest drawback is that it gives axially symmetric differential and integral worth curves. In practice, however, this rarely occurs in the UMLRR because the system is operated with the control blades banked at some axial position within the active fuel region. This is required to offset any excess reactivity in the system for operation at a just-critical condition -- as indicated above, the expected critical height for the initial LEU core configuration is 16.5 inches withdrawn. This situation leads to an axially asymmetric neutron flux distribution, with the peak flux occurring below the axial centerline.

The same situation is also encountered when performing blade worth calibrations, in that the remaining three blades are inserted into the core at some position while the worth of the fourth blade is being measured. This is required to maintain the system near critical and it always leads

to differential blade worth data that show a bottom-peaked distribution. The problem, of course, is that eqn. (1) cannot model this asymmetry; so the curve fits are never very good.

Although the current in-house procedures, with the use of eqn. (1) for the curve fits, has been in use since the startup of the UMLRR, it has been recognized for years that this is probably not the best approach for blade calibration at the UMLRR. With the HEU to LEU fuel conversion planned for the summer of 2000, the time was right to re-evaluate the blade worth calibration procedures to be used for the new LEU core. In fact, the computational need to address this concern was an important motivating factor for the development of the 3-D VENTURE model of the LEU core. In particular, the axial region layout within the current 3-D LEU model was chosen so that detailed simulations of the blade calibration procedure could be accomplished prior to the startup of the new core.

As an example, we will focus our detailed discussion on the analysis for Blade #1, but similar calculations have been completed for the other control blades and the regulating blade -- and, for completeness, the summary differential and integral worth data for all the blades are included here. The LEU315 3-D VENTURE model of the reference 21-element LEU core was used for all the calculations. The only difference among the various runs was the axial location of the control blades, with the regulating blade fixed at the full out position of 26 inches withdrawn. As indicated previously, the VENTURE model has 17 axial layers. The top three layers always have control present and the bottom three layers never have control. The middle 11 layers, covering a 26-inch range, vary their control state by simply changing the material composition to contain the homogenized control blade material (control in) or water (control out).

The Blade #1 differential worth simulations started with Blade #1 fully inserted and Blades #2, 3, and 4 banked at 18.9 inches withdrawn. Since the blades can only be moved in discrete increments consistent with the axial layer thickness in the 3-D VENTURE model, an exact critical state cannot be maintained within the computations. Instead, if  $k_{\text{eff}}$  was within  $\pm 1\%$  of unity, we considered this state nearly critical, and appropriate  $\% \Delta k/k$  data for each  $\Delta z$  change in the Blade #1 location were recorded. When  $k_{\text{eff}}$  fell outside this bound, Blades #2, 3, and 4 were re-banked to bring the system back to "critical". Using this logic, only one re-bank calculation was needed when Blade #1 was at 14.2 inches out, and the new location of the remaining three blades was 16.5 inches withdrawn.

In an attempt to mimic the actual measurements that are made in the UMLRR, where usually 4-7 actual data values are measured, only a subset of the available 12 blade locations were sampled in the current simulations. In particular, summary data for 9 different 3-D VENTURE  $k_{\text{eff}}$  calculations are contained in Table II. These data include computations for 8 different Blade #1 positions and a single re-bank calculation.

The raw data given in Table II for the Blade #1 simulations, as well as similar data for the other blades, were converted into a complete set of differential blade worth information for the reference 21-element LEU core. This summary information is given in Table III. This table shows the computed  $\% \Delta k/k$  per inch values that are associated with the midpoint of the interval traversed by the control blades and the regulating blade. Note that we have added two zero-worth data points at either end of the blade range, giving 9 data points for the subsequent fits for the differential worth curves. The "extra" endpoint data force the mathematical models to be better behaved at the ends.

**Table II Raw data for the simulated differential worth experiments for Blade #1.**

<b>Position #</b>	<b>Blade #1 distance withdrawn (inches)</b>	<b>Blades #2-4 distance withdrawn (inches)</b>	<b>3-D VENTURE <math>k_{eff}</math></b>
1	0.00	18.9	0.99294
2	4.18	18.9	0.99432
3	7.09	18.9	0.99736
4	11.8	18.9	1.00568
5	14.2	18.9	1.01025
Re-bank Blades 2-4	14.2	16.5	0.99997
6	18.9	16.5	1.00672
7	21.8	16.5	1.00887
8	26.0	16.5	1.00999

**Table III Simulated differential worth data for the reference UMLRR LEU core.**

<b>Point</b>	<b>Interval Midpoint (inches withdrawn)</b>	<b>Differential Worth (<math>\% \Delta k/k</math> per inch)</b>				
		<b>Blade #1</b>	<b>Blade #2</b>	<b>Blade #3</b>	<b>Blade #4</b>	<b>Reg. Blade</b>
1	0.00	0.000	0.000	0.000	0.000	0.000
2	2.09	0.033	0.037	0.041	0.042	0.008
3	5.64	0.105	0.116	0.131	0.135	0.022
4	9.46	0.177	0.187	0.221	0.226	0.032
5	13.00	0.192	0.194	0.239	0.245	0.033
6	16.54	0.143	0.139	0.181	0.184	0.023
7	20.36	0.073	0.071	0.095	0.098	0.011
8	23.91	0.027	0.025	0.036	0.037	0.004
9	26.00	0.000	0.000	0.000	0.000	0.000

As indicated previously, one aspect of this study was to focus on the goodness of the actual mathematical model used to fit the discrete differential worth data. Clearly, we want to study the existing methodology that uses eqn. (1) to represent the data. Because of the rather awkward symmetry constraint associated with eqn. (1), however, we also decided to try a general cubic polynomial model, which, of course, does not have a formal axial symmetry requirement. Finally, after some trial and error tests with other models, we also decided to use a combination model, which simply sums a cubic polynomial and sinusoid, to see if we could minimize observed weaknesses in the separate models. Thus, three mathematical models were tested as possible candidates for fitting the differential worth data, as follows:

**Model A Theoretical Model**

$$\frac{d}{dz} \rho(z) = a_1 \left( 1 - \cos \left( \frac{2\pi z}{H} \right) \right) \quad (1)$$

**Model B Cubic Polynomial**

$$\frac{d}{dz} \rho(z) = b_1 + b_2 z + b_3 z^2 + b_4 z^3 \quad (2)$$

**Model C Combined Polynomial and Sinusoid**

$$\frac{d}{dz} \rho(z) = c_1 + c_2 z + c_3 z^2 + c_4 z^3 + c_5 \cos \left( \frac{2\pi z}{H} \right) \quad (3)$$

where H is the maximum blade traverse. Note that the units for differential worth are %  $\Delta k/k$  per inch, since these are the units used routinely by the UMLRR operations staff. The integral worth versus position,  $\rho(z)$ , is also computed, and this is simply calculated by taking the integral of eqns. (1)-(3).

A series of fits using the models given in eqns. (1)-(3) with the differential worth data from Table III were made with the assistance of a short Matlab code. The Matlab script file computes the best set of coefficients for each mathematical model, does some quantitative analysis to indicate the goodness of the fit, and then plots the differential and integral worth curves. Figures 7-11 represent the result of this exercise, with each figure showing both the fitted differential worth profile and the resultant integral worth curve for the particular control or regulating blade of interest.

Focusing first on the differential curves, we see that, of the models tested, the combined model (Model C with the cubic polynomial plus sinusoid) gave the best fit to the simulated worth data. All three models have the expected rough “bell-shaped” behavior, but only Model C was able to retain the “wings” at the ends of the blade and accurately represent the slightly “bottom-peaked” nature of the differential worth profile. In addition, the coefficient of determination (the COD is a measure of the goodness of the fit with unity being a perfect fit) was greater than 0.99 for Model C for all five blades. The CODs for the other models were generally about 0.95 or less. This quantitative measure and a simple visual inspection of the plots clearly indicate that Model C, with the combined polynomial and sinusoid, should be the mathematical model of choice for fitting measured blade worth data at the UMLRR.

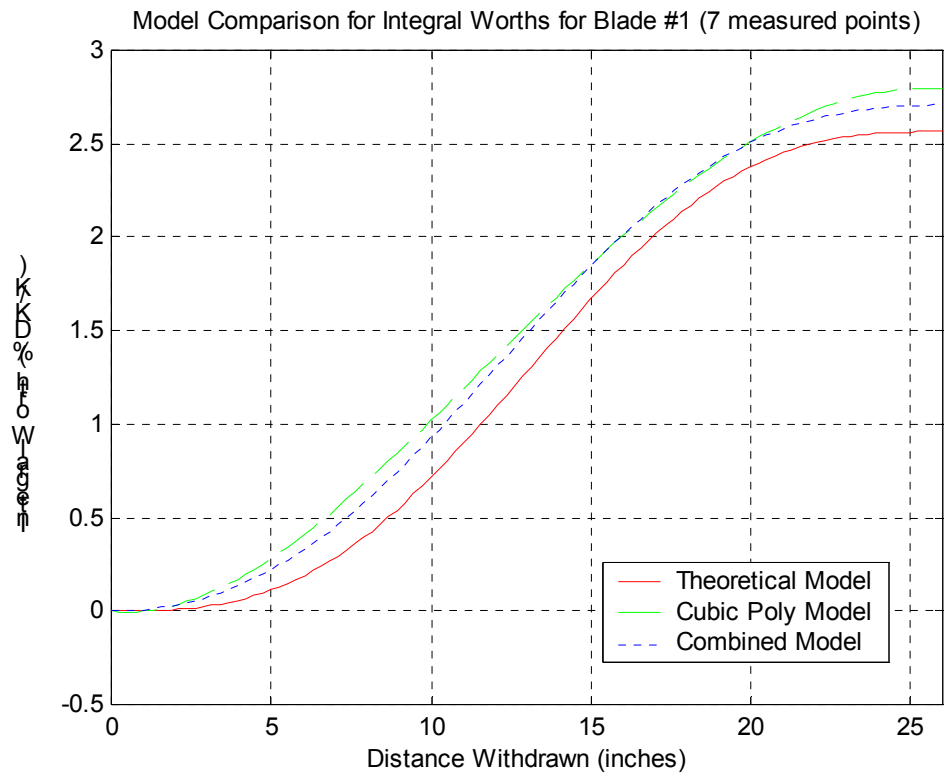
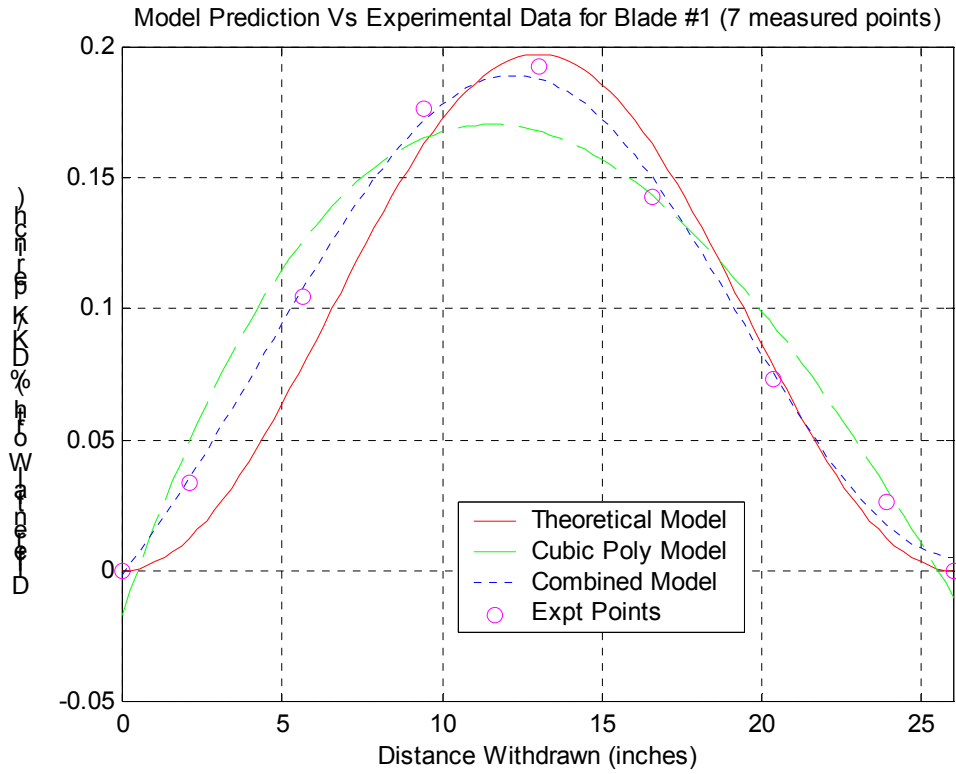


**Fig. 7 Differential and integral worth curves for Blade #1.**

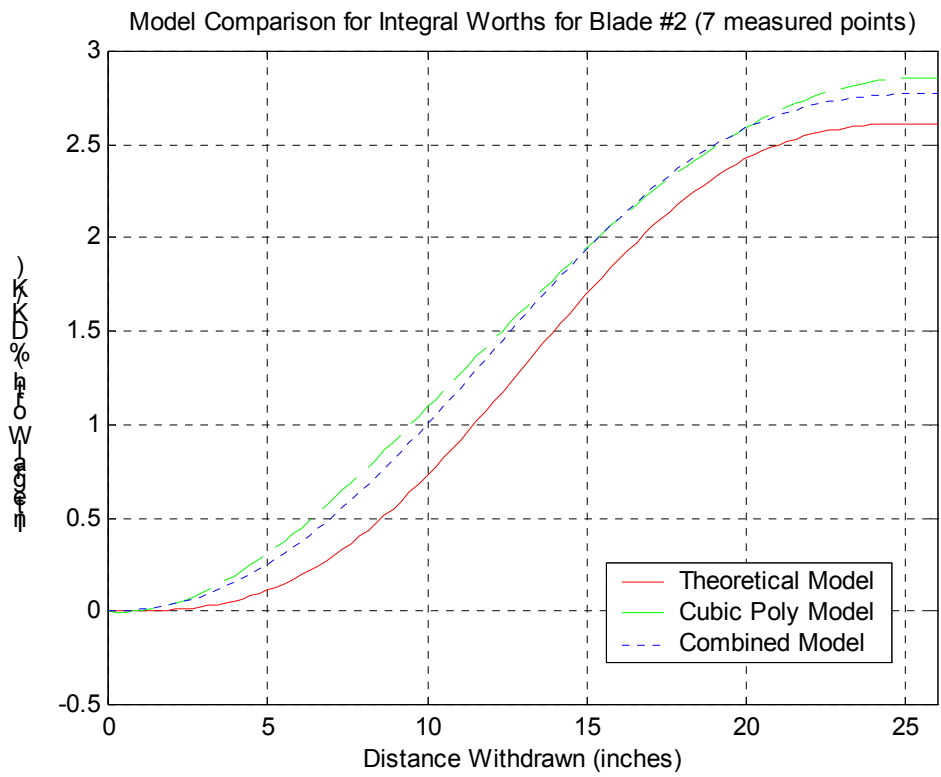
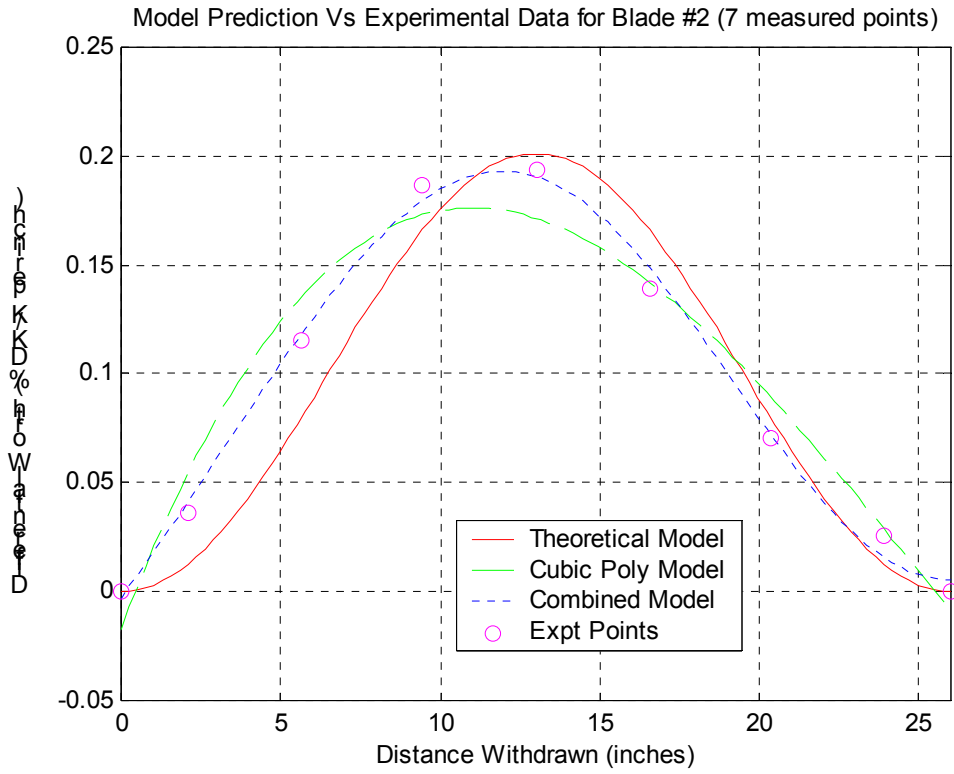


**Fig. 8 Differential and integral worth curves for Blade #2.**

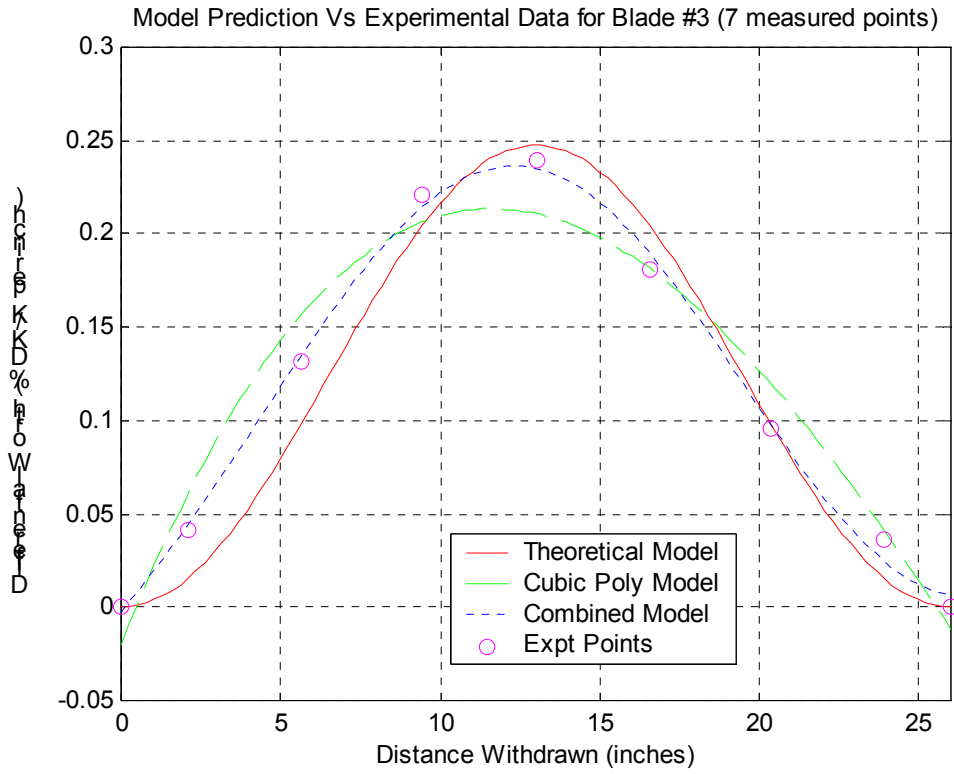


**Fig. 9 Differential and integral worth curves for Blade #3.**

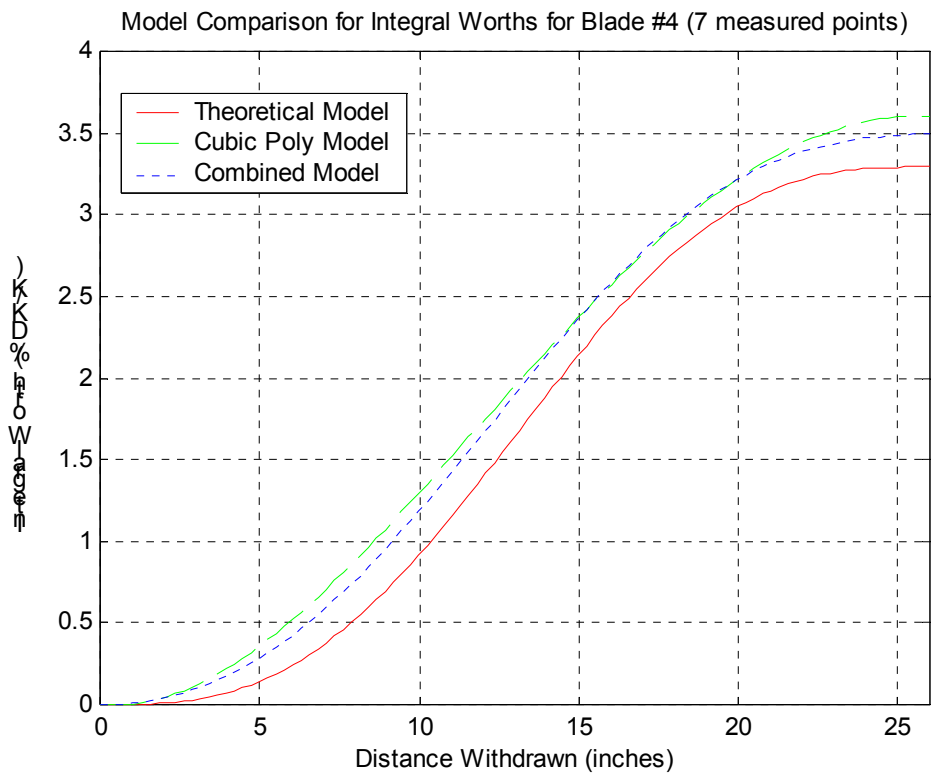
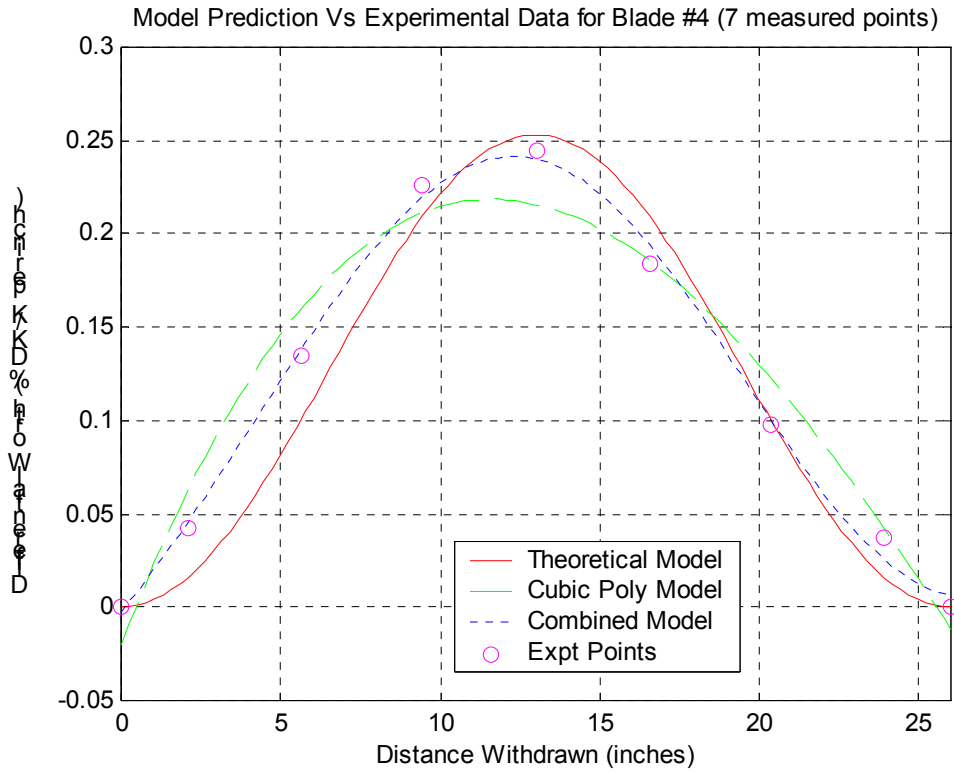


**Fig. 10 Differential and integral worth curves for Blade #4.**

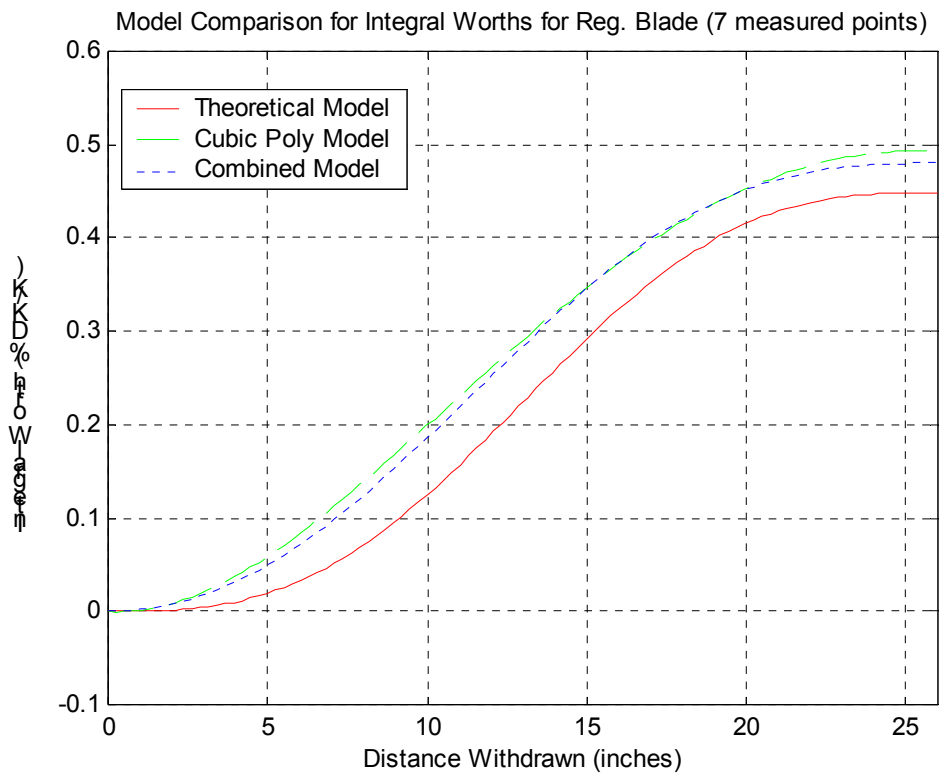
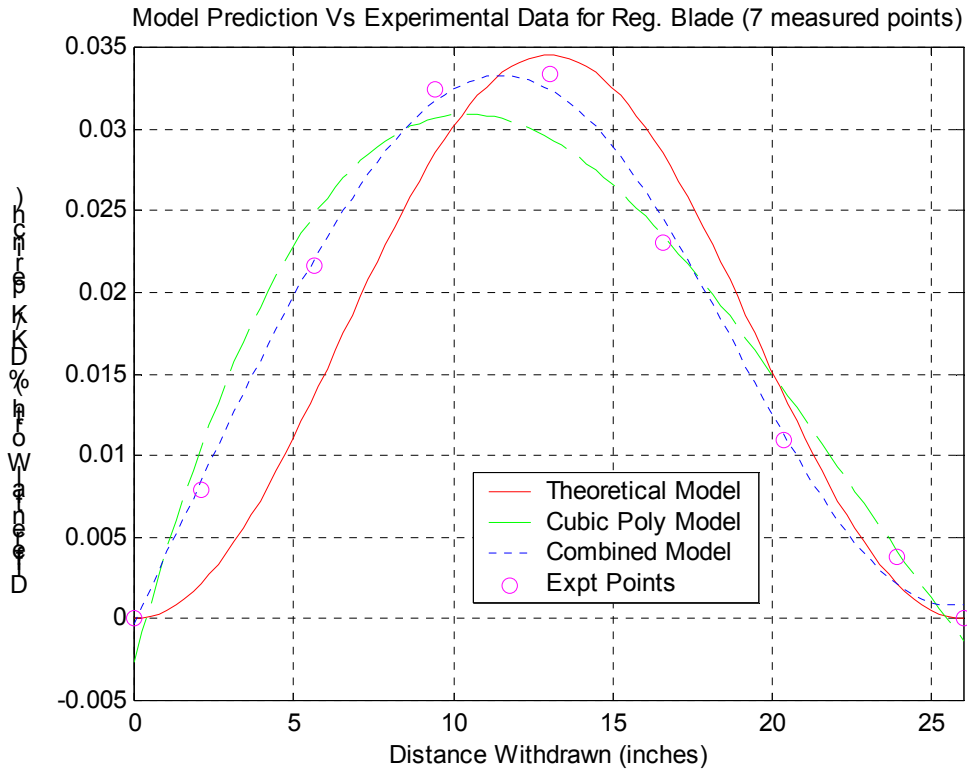


**Fig. 11 Differential and integral worth curves for the Regulating Blade.**

The above results strongly suggest that the current use of Model A should be discontinued, and that Model C should be incorporated within the UMLRR blade calibration procedure for the new LEU core. This recommendation, along with the full set of simulated differential and integral blade worth curves shown here, represent new information that should be quite useful during the actual startup tests for the new LEU core.

Finally, we note that the total worth of the individual blades is simply the value of the integral worth evaluated at the fully withdrawn position (at 26 inches in Figs. 7 - 11). These total worths have already been tabulated and discussed previously (see the last column of blade worth data in Table I). These data agree well with our simple 2-D control-in versus control-out VENTURE blade worth calculations. The data for the four large control blades are expected to be quite representative of the actual values observed in the physical system. The regulating blade worth uncertainty, however, is expected to be much larger, and a 20% bias has already been applied to the data shown in Table I. Thus, all the blade worth values in Table I are probably quite reasonable.

### CRITICAL LOADING SIMULATION

A 21-element core with 19 full fuel elements and 2 partial elements has already been chosen as the best candidate for the initial startup of the LEU-fueled UMass-Lowell research reactor (UMLRR).<sup>3</sup> As indicated above, both 2-D and 3-D VENTURE models have also been developed and these have been used to predict a variety of neutronic characteristics within the new core. A top view of the material layout for the reference core is shown in Fig. 1 (see pg. 4) along with a legend to help identify the various components within the system. This figure depicts the final goal of an initial loading procedure.

With the desired startup configuration known, we focused our attention on the simulation of the initial loading sequence needed to arrive at this end goal. A set of formal in-house procedures is used by the operations staff when performing a critical loading for a new configuration. The basic idea is to carefully monitor the subcritical multiplication associated with each new configuration as one goes from only a few elements towards a configuration that leads to a critical system. As the number of fuel elements in the core increases, the subcritical multiplication increases; eventually approaching infinity as a critical configuration is reached.

In monitoring a particular critical loading sequence, one often generates the so-called 1/M line for each step in the sequence. The neutron population and detector count rate are proportional to the neutron source strength and inversely related the degree of subcriticality given by  $1-k$ , where  $k$  is the standard neutron multiplication factor. Thus, we can represent the initial count rate for some source-detector configuration as<sup>13</sup>

$$C_0 = \frac{\alpha_0 S}{1 - k_0} \quad (4)$$

where  $\alpha_0$  is a proportionality constant. If the fuel configuration is changed, possibly by adding additional assemblies at the  $i^{\text{th}}$  step of a critical loading sequence, eqn. (4) becomes

$$C_i = \frac{\alpha_i S}{1 - k_i} \quad (5)$$

where  $k_i$  is the multiplication factor associated with the  $i^{\text{th}}$  core configuration. The subcritical multiplication for this configuration is defined from the ratio of the current count rate and initial count rate, or

$$M_i = \frac{C_i}{C_0} \quad (6)$$

Substituting eqns. (4) and (5) into the “inverse” of this expression gives

$$\frac{1}{M_i} = \frac{\alpha_0}{\alpha_i} \frac{1 - k_i}{1 - k_0} = \beta_i (1 - k_i) \quad (7)$$

where  $\beta_i$  is simply another proportionality constant. The important feature here is that the inverse subcritical multiplication factor,  $1/M$ , is approximately a linear function of the neutron multiplication factor,  $k$ . In particular, a plot of  $1/M$  using two known values can be easily extrapolated to the  $1/M = 0$  point -- which gives a prediction of when the system will be critical (i.e.  $k = 1$ ).

Our approach to the numerical simulation of the initial critical loading experiment for the new LEU core involved the computation of the neutron multiplication factor,  $k_i$ , for several different loading configurations. With this information, a standard  $1/M$  plot could be generated, simulating what might be expected during the actual approach to critical for the new LEU core. The data for the plot were generated with a 2-D VENTURE  $k_{\text{eff}}$  calculation for each of the different assembly configurations. Several 3-D computations were also performed at various stages, but these data were used only to estimate any 2-D versus 3-D differences that might effect the prediction of the critical loading.

The calculations started by loading the core periphery with an arrangement of graphite reflectors and radiation basket assemblies that is consistent with the final proposed LEU215/LEU315 core configuration as shown in Fig. 1. This arrangement leaves 22 centrally located grid positions available for the placement of full and partial fuel assemblies and the central flux trap irradiation facility.

We decided to initially load only full fuel elements starting in the central core region. New assemblies are then added in a systematic manner, trying to maintain as much symmetry as possible, until the core is nearly critical. At this point, the full fuel assembly in D5 is removed and replaced with the flux trap assembly. In addition, the full fuel elements in C5 and E5 are exchanged with two partial assemblies. Both these moves decrease the core multiplication factor,  $k_{\text{eff}}$ , and increase the inverse subcritical multiplication,  $1/M$ , in the system. After this configuration change, the normal systematic loading of full fuel assemblies is continued until a critical core is reached.

A summary of the actual loading sequence and the data obtained from the VENTURE calculations is given in Table IV. Also displayed in Fig. 12 is a visual diary of the core arrangement associated with each step of the simulated loading experiment. Here we see that a sequence of 15 calculations were made, starting with 5 fuel assemblies in the C5, D4, D5, D6, and E5 positions. Two fuel assemblies were added per step for the first several steps and then only one element was added at each step as the system got closer to critical -- and this approach is fully consistent with standard procedures which emphasize a slow careful approach to criticality.

**Table IV Summary data from the VENTURE critical loading calculations.**

Case ID	# of Elements	Positions Added	$k_{\text{eff}}$ (3D)	$k_{\text{eff}}$ (2D)	1/M = (1-k)
cl 1	5	C5,D4,D5,D6,E5	--	0.74760	0.252
cl 2	7	C4,E6	--	0.82280	0.177
cl 3	9	C6,E4	0.88986	0.89152	0.108
cl 4	11	D3,D7	--	0.93372	0.066
cl 5	13	C3,E7	--	0.96206	0.038
cl 6	14	C7	--	0.98134	0.019
cl 7	15	E3	0.99868	0.99367	0.006
cl 8	14	Replace FA with FT in D5	--	0.95656	0.043
cl 9	14	Replace FA with PA in C5,E5	0.93588	0.93309	0.067
cl 10	15	D8	--	0.94851	0.052
cl 11	16	F5	--	0.96242	0.038
cl 12	17	B5	--	0.97476	0.025
cl 13	18	F6	0.99527	0.99138	0.009
cl 14	19	B4	1.00687	1.00302	-0.003
cl 15	21	B6, F4	1.03672	1.03256	

Note that, at Step 7, 15 full fuel assemblies are loaded into the central 3x5 region of the core. This configuration, with 7 grid positions still containing only water, is nearly critical --  $k_{\text{eff}}$  from the 3-D calculation is 0.999. Thus, it appears that the minimum critical size associated with the new LEU fuel elements is roughly 15-16 elements with mostly water reflection on the periphery.

However, the final configuration of interest contains a central flux trap facility and two partial assemblies. Thus, at this point, it was decided that Steps 8 and 9 would incorporate these assemblies into the developing core configuration. These modifications decreased reactivity substantially, allowing the critical loading process to continue towards the final desired configuration. After 5 more steps, bringing the total assembly count to 17 full elements and 2 partial elements, the current calculations predict that the system will be slightly supercritical (with no control inserted). Within the limitations of the VENTURE modeling and within the context of the configurations described in Fig. 12, criticality should be reached with about 18-20 elements in the core, with our best estimate showing that criticality is achieved with between 18 and 19 elements loaded (includes two partial elements).

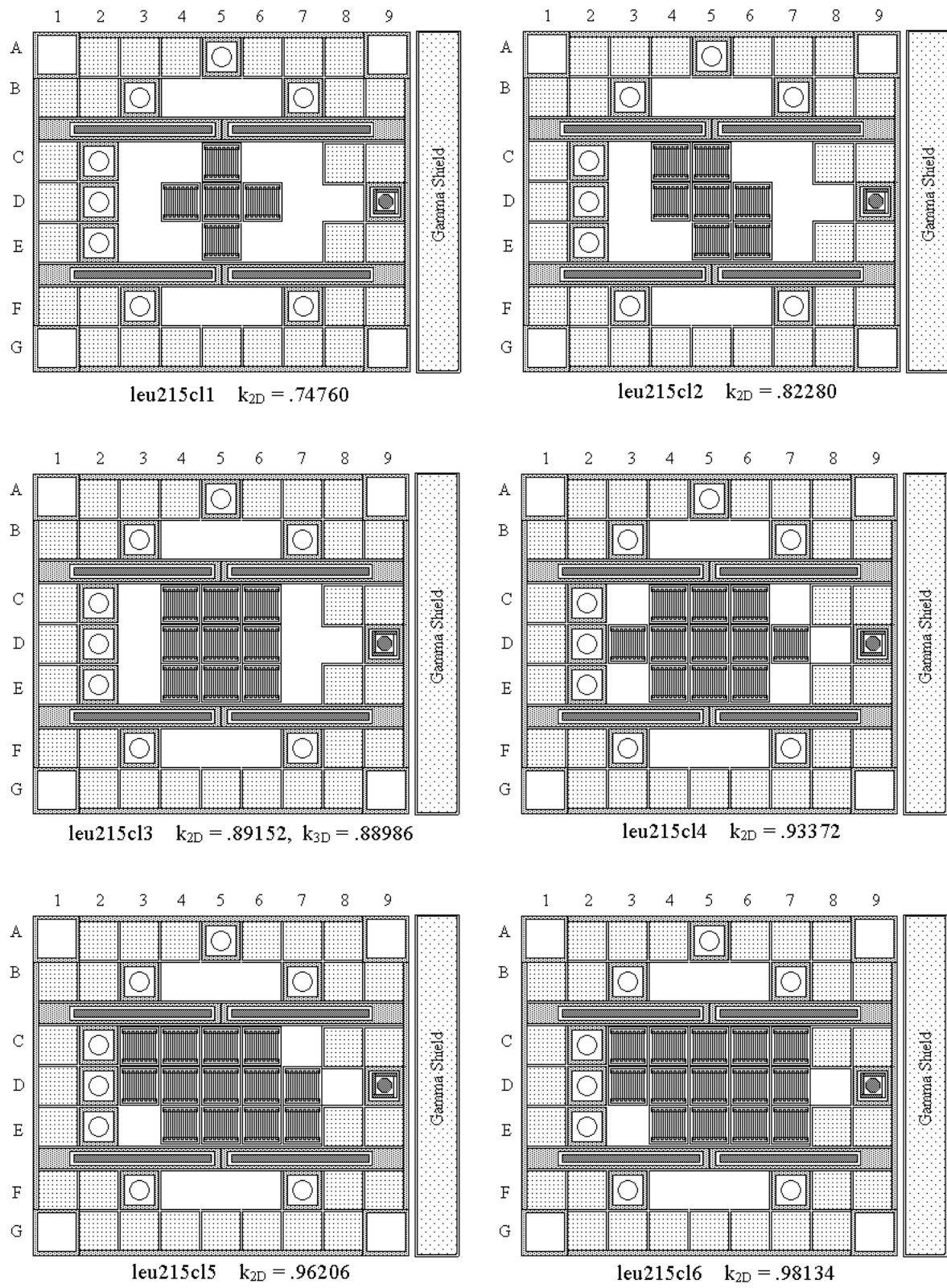
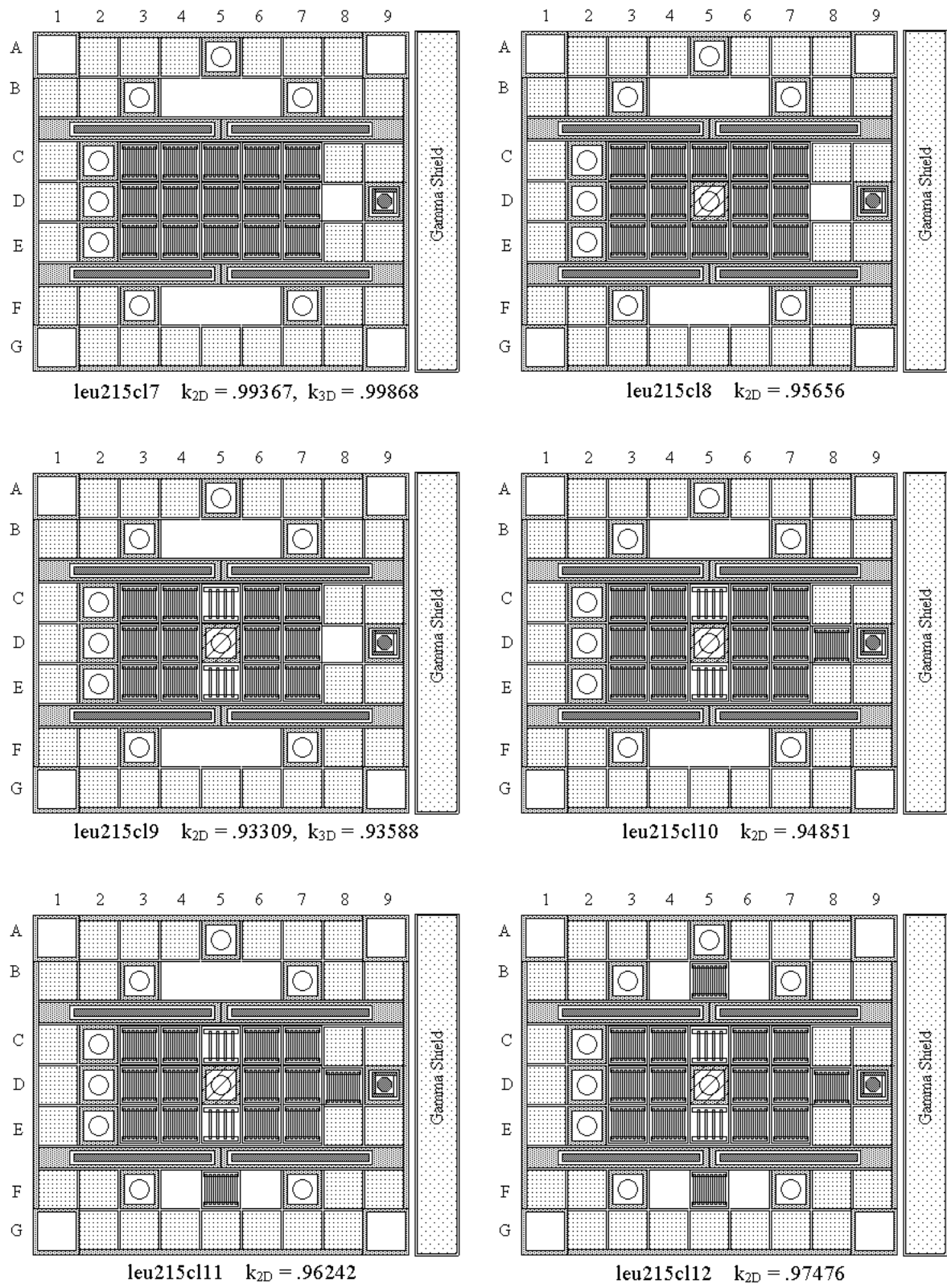
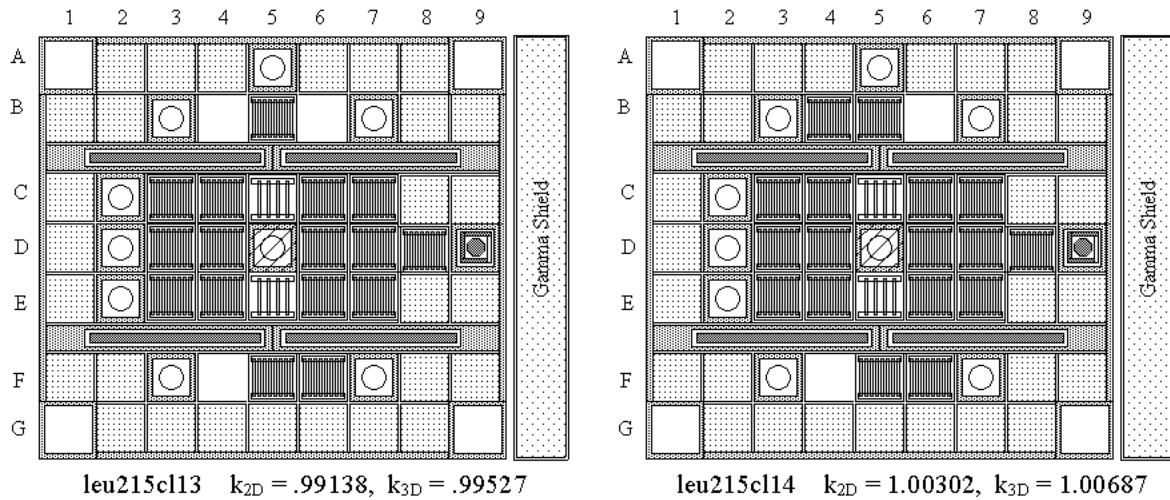


Fig. 12 Core layout at each step of the critical loading sequence.



**Fig. 12 Core layout at each step of the critical loading sequence (continued).**



**Fig. 12 Core layout at each step of the critical loading sequence (continued).**

The sequence of 14 steps that lead to a slightly supercritical core is summarized in Table IV and in the 14 core configuration maps displayed as part of Fig. 12. These data summarize quite nicely the simulated loading calculations performed here. This simulated experiment was performed to help guide the actual critical loading once the new LEU fuel arrives at UMass-Lowell. During the actual loading, however, the core  $k_{\text{eff}}$  is not directly available to the operators. However, using a ratio of count rates from different configurations, the subcritical multiplication factor in eqn. (6) is easily estimated. With this information, the standard  $1/M$  plot can be used to monitor the loading sequence and predict when criticality will occur.

With the computed  $k_{\text{eff}}$  from the 2-D VENTURE calculations, eqn. (7) with  $\beta_i = 1$  was used to determine a sequence of  $1/M$  values consistent with the individual steps in the proposed loading scheme. The  $1/M$  values are given in Table IV and plotted, along with straight lines that represent linear extrapolations to the  $1/M = 0$  point, in Fig. 13. This simulated  $1/M$  plot should be very similar to the one actually generated as part of the real critical loading of the LEU-fueled UMLRR. It is easy to see that the system with 15-16 fresh fuel assemblies represents a critical system -- since  $1/M$  approaches zero. Also, it is easy to see the discontinuity that occurs with the interchange of full fuel in D5 and in C5 + E5 with the flux trap and two partial fuel assemblies. After this abrupt increase in  $1/M$  (or decrease in  $k_{\text{eff}}$ ), criticality is again approached systematically until a slightly supercritical system is obtained with 19 elements loaded (17 full and 2 partial).

The final step in the loading procedure adds two additional full fuel assemblies into locations B6 and F4 to obtain the initial startup core for the LEU-fueled UMLRR. This configuration is shown in Fig. 1 and it has an excess reactivity of about 3.3 - 3.7%  $\Delta k/k$  based on the 2-D and 3-D VENTURE calculations, respectively. With the 3-D model, the estimated critical blade height needed to offset this excess reactivity is about 16.5 inches withdrawn -- this estimate assumes that the regulating blade is fully out. This configuration, with the blades partially inserted, is expected to be a reasonable approximation to the actual operational configuration for the LEU startup core.

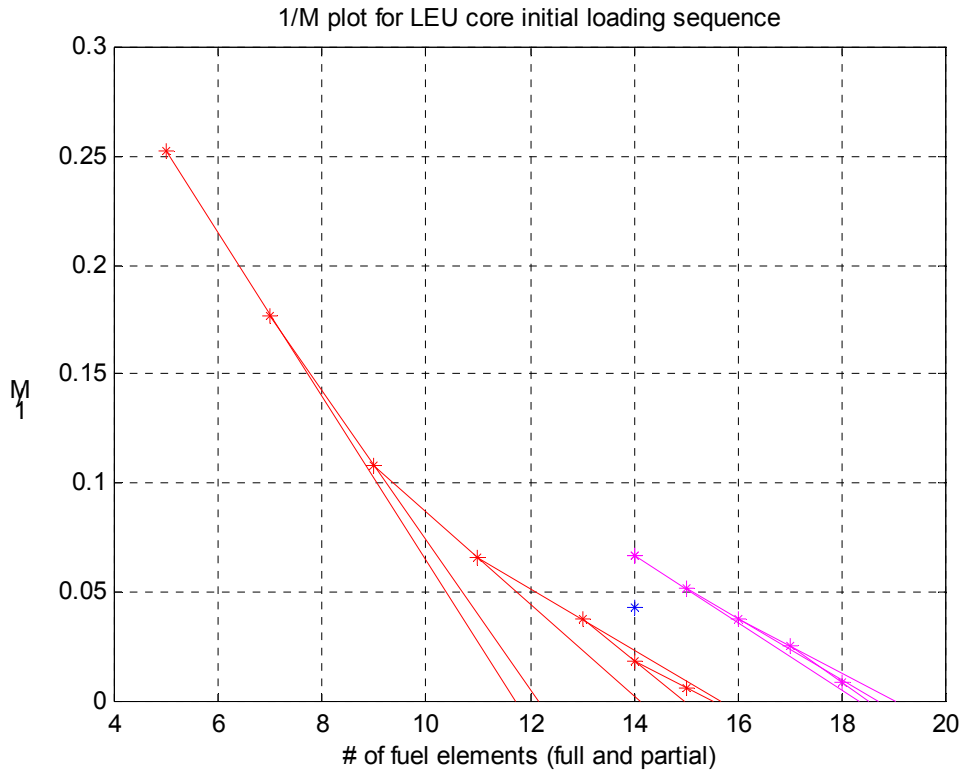


**Fig. 13** 1/M plot for the proposed initial critical loading sequence.

To summarize briefly, this analysis has identified a candidate sequence of steps that should lead to the desired operating configuration in a systematic predictable manner. The overall plan is broken into two sequences that are separated by a rather large decrease in reactivity when three full fuel assemblies are replaced with the central flux trap and two partial elements. This two-stage procedure was adopted to guarantee a well-behaved 1/M plot over the full range of assemblies loaded. The first sequence predicts criticality with about 15-16 full fuel assemblies and, after reducing the reactivity of the elements in the C5, D5, and E5 positions, criticality is not achieved until 18-19 total elements are loaded. The loading of the two additional full fuel elements gives about 3.5% excess reactivity for normal operation of the facility. This excess reactivity is offset during operation at a just-critical condition by inserting the four large control blades to about 16.5 inches withdrawn. This simulation of the critical loading process, including the data in Table IV, the core maps in Fig. 12, and the simulated 1/M plot in Fig. 13, should be an invaluable guide during the actual initial loading of the LEU core.

### SUMMARY AND FUTURE WORK

The work reported here and in Ref. 7 has developed a substantial computational infrastructure and a large database of information for the new UMLRR LEU core. We now have a series of computer models that can help answer many of the common questions that arise during routine operation of the UMLRR. We have reasonable estimates of the excess reactivity and total blade worths for the new reference 21-element LEU core, an initial loading sequence has been

proposed and simulated, differential and integral blade worth data have been simulated and a new curve fitting procedure for use with the experimentally determined differential worth data has been proposed and, finally, the data reported in Ref. 7 help to characterize the radiation environments that are expected within several of the experimental facilities in the UMLRR. Certainly the computational models have inherent limitations, but the results generated here (with some notable exceptions like the small sample worth calculation in the 3-D VENTURE model) should paint a reasonably accurate picture of expected behavior of the new LEU core. However, definitive validation of the model predictions is nearly impossible until direct comparisons to measured data are made. Thus, our studies will not be complete until rigorous comparisons of our model prediction capability and the measured data from the operating facility are performed. Hopefully this will take place during the later half of 2000 when the new LEU core is operational and experimental data begin to become available.

In addition to the model validation efforts that are certainly required as future work, there are two more model development issues or deficiencies that should be resolved as part of future studies. As mentioned previously, the current VENTURE models cannot accurately address the reactivity worth of a small sample inserted into the radiation basket or flux trap facilities. The 2-region basket model incorporated into the overall VENTURE core models requires that the sample be homogenized within the existing central zone geometry. The smearing or homogenization of a poison sample within a much larger volume often leads to serious over prediction of the sample worth, even when the appropriate atom density reduction is treated. The current VENTURE zone geometry could be reduced in size to try to minimize the homogenization problem but, unfortunately, we may never be able to eliminate this problem completely -- because the required mesh sizes could become prohibitively small.

The prediction of small sample worths is particularly important in the new LEU core because of the central flux trap facility. It is expected that the worths in this location could become quite large, even for samples that are used routinely in the radiation basket region. We expect that an increase in worth of about a factor of 3 to 5 or more may be observed when a given sample is moved from the D2 position to the D5 position. This means that an accurate prediction of the sample worth in the flux trap will be required to assure that appropriate Technical Specification limits for movable experiments are not exceeded -- and the current VENTURE model is simply not suitable for this task. Thus, additional efforts are needed to enhance and validate an existing (but very preliminary) MCNP model of the LEU-fueled UMLRR.<sup>3</sup> A well documented and fully validated MCNP model, with its explicit geometry capability, could easily handle the prediction of small sample worths, and it could be generally useful for complete pre-analysis of any new proposed experimental configuration. Such capability would be a tremendous asset to complement our existing modeling tools, and with the potential for high reactivity worths in the flux trap location, it could easily become an essential component of the safety review that is required for any new experiment within the facility.

The final modeling concern that should be given priority for future work relates to the extension of our current modeling capability to allow analysis beyond the initial LEU core configuration. The VENTURE code has integrated fuel burnup capability within the BURNER module. Our existing models can easily be enhanced so that fuel depletion calculations can be performed to allow core follow and prediction capability well into the future. Developing a cross section library that is suitable for depletion analysis is always a challenge, but this task simply requires extension of the procedures and tools used to generate the cross sections for the current study. In

short, fuel depletion capability within the existing models would allow us to continue our analytical support of the UMLRR for the next 20 - 30 years or more. This would certainly be beneficial for continued operational support throughout the life of the facility and it also increases the overall usefulness and cost-benefit of all the capability developed as part of the current study.

### ACKNOWLEDGEMENTS

This work was supported by a Department of Energy grant under Project #14-08239-F through the University of Massachusetts Lowell Research Foundation.

### REFERENCES

1. R. S. Freeman, "Neutronics Analysis for the Conversion of the ULR from High Enriched Uranium to Low Enriched Uranium Fuel," MS Thesis, Chemical and Nuclear Engineering, University of Lowell (May 1991).
2. "FSAR Supplement for Conversion to Low Enrichment Uranium (LEU) Fuel," Document submitted for review by the NRC for conversion of the UMass-Lowell Research Reactor (May 1993).
3. J. R. White and R. D. Tooker, "Modeling and Reference Core Calculations for the LEU-Fueled UMass-Lowell Research Reactor," ANS 1999 Winter Meeting, Long Beach, CA (Nov. 1999).
4. "VENTURE-PC - A Reactor Analysis Code System," Radiation Safety Information Computational Center, CCC-654 (1997).
5. "DOORS3.1 - One, Two, and Three Dimensional Discrete Ordinates Neutron/Photon Transport Code System," Radiation Safety Information Computational Center, CCC-650 (1996).
6. "MCNP-4B - Monte Carlo N-Particle Transport Code System," Radiation Safety Information Computational Center, CCC-660 (1997).
7. J. R. White, et. al., "Preliminary Characterization of the Irradiation Facilities within the LEU-Fueled UMass-Lowell Research Reactor," Topical Meeting on Advances in Reactor Physics and Mathematics and Computation (these proceedings), Pittsburgh, PA (May 2000).
8. "SCALE 4.3 - Modular Code System for Performing Standardized Computer Analyses for Licensing Evaluation for Workstations and Personal Computers," Radiation Safety Information Computational Center, CCC-545 (1997).
9. "VITAMIN-B6 - A Fine-Group Cross Section Library Based on ENDF/B-VI Release 3 for Radiation Transport Applications," Radiation Safety Information Computational Center, DLC-184 (1996).
10. "Proposed Technical Specifications for the University of Massachusetts Lowell Reactor with Low Enrichment Fuel," Document submitted for review by the NRC for conversion of the UMass-Lowell Research Reactor (May 1993).

11. J. P. Phelps, "Startup Report for the LTI Reactor," University of Lowell (May 1975).
12. J. R. Lamarsh, *Introduction to Nuclear Engineering*, Addison-Wesley Publishing Company (1983).
13. R. R. Burn, "Introduction to Nuclear Reactor Operations," Copyright 1982 by Reed Robert Burn.